

Gümüş Nanoparçacıklarına Çinko Katkılanmasının Toksik Organik Boyaların Bozunmasının Artırılmasına Etkilerinin İncelenmesi

Merve AKBAYRAK^{1,3}  Ümran ATA^{2,3}  Tuğba Nur ASLAN^{2,3*} 

¹ Necmettin Erbakan University, Faculty of Science, Department of Biotechnology, Konya, Türkiye

² Necmettin Erbakan University, Faculty of Science, Department of Molecular Biology and Genetics, Konya, Türkiye

³ Necmettin Erbakan University, Science and Technology Research and Application Center (BITAM), Konya, Türkiye

Makale Bilgisi

ÖZET

Geliş Tarihi: 08.05.2024
Kabul Tarihi: 02.10.2024
Yayın Tarihi: 30.04.2025

Anahtar Kelimeler:

Çinko,
Gümüş,
Metil Turuncusu,
Metilen Mavisini,
Nanoparçacık.

Bu çalışmada, gümüş nanoparçacıkların katalitik verimliliğini artırmak amacıyla, Çinko katkılı Gümüş Nanoparçacıklar (Zn katkılı Ag NP'ler) sentezlenmiştir. Polygonum cognatum özütü ile çinko katkılama oranı sistematik olarak değiştirilerek (çıplak Ag NP, %1,6 Zn katkılı Ag NP ve %9,0 Zn katkılı Ag NP) kontrollü bir yeşil sentez yapılmıştır. Endüktif Eşleşmiş Plazma Optik Emisyon Spektroskopisi (ICP-OES), Taramalı Geçirimsiz Elektron Mikroskopisi (STEM), Enerji Dağılımlı X-Işım Spektroskopisi (EDS), X-ışım Floresansı (XRF), X-ışım Kırınımı (XRD) ve Fourier Dönüşümlü Kızılötesi Spektroskopisi (FTIR) analizleri, NP'lerin oluşumunu, elemental içeriğini, kristal yapısını ve Zn'nin Ag NP matrisine etkili bir şekilde dahil edildiğini doğrulamıştır. Yeşil sentezlenmiş Zn katkılı Ag NP'lerin, indirgeyici ajan olarak sodyum borohidrit (NaBH₄) çözeltisi kullanılarak metil turuncusunun (MO) ve metilen mavisinin (MB) bozunmasındaki katalitik aktiviteleri araştırılmıştır. Sonuçlara göre, Zn katkılı Ag NP'ler çıplak Ag NP'lere kıyasla üstün katalitik performans sergilemiştir. Sonuçlar, %9,0 Zn katkılı Ag NP'nin MO'yu 15 dakika içinde 0,2199 dk⁻¹ hız sabiti (kapp) ve 1,65 x 10⁻³ mol.g⁻¹ dk⁻¹ devir frekansı (TOF) ile %96,56 oranında parçaladığını göstermektedir. MB degradasyonunda parçalama yüzdesi, 0,4445 dk⁻¹ kapp ve 2,54 x 10⁻³ mol.g⁻¹ dk⁻¹ TOF ile 10 dakikada %98,38'e ulaşmıştır. Her iki boya için de Zn katkılama miktarının %1,6'dan %9,0'a çıkarılması reaksiyon sürelerini büyük ölçüde kısaltmış ve bozunma verimliliğini artırmıştır. 9.0 % Zn katkılı Ag NP'lerin toksik organik boyaların hızlı ve verimli bir şekilde bozunması için oldukça etkili katalizörler olduğu bulunmuştur. Bu çalışmanın bulguları, çevresel arıtma ve diğer uygulamalar için daha etkili ve özelleştirilebilir katalitik malzemelerin geliştirilmesini sağlayacak olan çinko katkılama yoluyla gümüş nanopartiküllerin etkinliğinin ayarlanabilirliği hakkında değerli bilgiler sağlamaktadır.

Influence of Zinc Doping Ratio on Silver Nanoparticles Synthesized via Green Method for Enhanced Catalytic Degradation of Toxic Organic Dyes

Article Info

ABSTRACT

Received: 08.05.2024
Accepted: 02.10.2024
Published: 30.04.2025

Keywords:

Metyl Orange,
Methylene Blue,
Nanoparticles,
Silver,
Zinc.

Zinc doped Silver Nanoparticles (Zn doped Ag NPs) were synthesized in this study to improve catalytic efficiency of Ag NPs. A controlled green synthesis was achieved with Polygonum cognatum extract by systematically varying zinc doping ratio (bare Ag NP, 1.6% Zn-doped Ag NP, and 9.0% Zn-doped Ag NP). Inductively Coupled Plasma Optical Emission Spectroscopy (ICP-OES), Scanning Transmission Electron Microscopy (STEM), Energy Dispersive X-ray Spectroscopy (EDS), X-ray Fluorescence (XRF), X-ray Diffraction (XRD), and Fourier Transform Infrared Spectroscopy (FTIR) analyses verified the NP formation, its elemental content, crystal structure and successful incorporation of Zn into the Ag NP matrix. The catalytic activity of green synthesized Zn doped Ag NPs was investigated in the degradation of methyl orange (MO) and methylene blue (MB) using sodium borohydride (NaBH₄) as a reducing agent. According to results, Zn doped Ag NPs exhibited superior catalytic performance compared to bare Ag NPs. The results indicate that the 9.0% Zn-doped Ag NP degraded MO 96.56% in 15 minutes at a rate constant (kapp) of 0.2199 min⁻¹ and turnover frequency (TOF) of 1.65 x 10⁻³ mol.g⁻¹ min⁻¹. In MB degradation, it reached 98.38% in 10 minutes with a kapp of 0.4445 min⁻¹ and a TOF of 2.54 x 10⁻³ mol.g⁻¹ min⁻¹. For both dyes, increasing the doping amount of Zn from 1.6% to 9.0% greatly shortened reaction times and improved degradation efficiency. 9.0% Zn doped Ag NPs were found highly effective catalysts for the rapid and efficient degradation of toxic organic dyes. The findings of this study provide valuable insights into the tunability of silver nanoparticles' activity through zinc doping, which will enable the development of more effective and customizable catalytic materials for environmental treatment and other applications.

To cite this article:

Akbayrak, M., Ünüvar, Ü. & Aslan, T.N. (2025). Influence of zinc doping ratio on silver nanoparticles synthesized via green method for enhanced catalytic degradation of toxic organic dyes. *Necmettin Erbakan University Journal of Science and Engineering*, 7(1), 56-76. <https://doi.org/10.47112/neufmbd.2025.75>

*Corresponding Author: Tuğba Nur Aslan, taslan@erbakan.edu.tr



This article is licensed under a Creative Commons Attribution-NonCommercial 4.0 International License (CC BY-NC 4.0)

INTRODUCTION

Environmental sustainability and resource management are among the most significant issues in today's world. Environmental treatment plays a vital role in protecting and improving natural resources as a comprehensive process. Environmentally friendly treatment efforts against some environmental pollutions may contribute to the sustainability of water and other resources such as air and soil [1]. Organic compounds such as methylene blue (MB) and methyl orange (MO) dyes are widely used indicators in industrial applications, however their environmental impact is also significant [2]. MO is used primarily in the colorant and dye industry and can cause environmental pollution by entering water systems through wastewater. MB is another indicator compound used in the textile, paper, and pharmaceutical industries and has an environmental impact by contaminating water systems [3]. Both compounds can cause toxic effects in aquatic ecosystems and can be harmful to various living organisms, especially in case of prolonged exposure to these substances [4]. Therefore, it is important to develop environmental management strategies for these organic indicator compounds considering their impact on the environment [5]. Conventional water treatment methods often fall short in effectively removing a wide range of pollutants, leading to a growing interest in advanced catalytic processes. Catalytic degradation of pollutants with the use of nanoparticles as catalysts can be considered as a sustainable and promising approach due to their high surface area and unique chemical properties for the removal of harmful substances [6-8].

Silver nanoparticles (Ag NPs) with unique properties, may have excellent catalytic performances, thus they have attracted attention for studies on improving catalytic processes [9]. The most important characteristics of Ag NPs are their high reactivity towards organic molecules thanks to their large surface area/volume ratio and their optical properties arising from metal surface plasmon resonances (SPR) [10]. Ag NPs efficiently absorb light and release their free electrons stimulatingly due to their SPR [11]. Therefore, the catalytic utility of Ag NPs holds great potential in environmental treatment and energy conversion [12]. However, it was revealed that the catalytic activities of NPs can be improved by metal doping due to a synergetic effect of two metals' intrinsic catalytic properties [13]. For better catalytic properties, doping Ag NPs with other metals, such as zinc (Zn), has been proposed [14]. Zn doping can modify the electronic properties and surface chemistry, thereby altering SPR properties of Ag NPs [15]. SPR causes concentrated electromagnetic fields on the surface, which increase the catalytic activity by creating a suitable environment for catalytic reactions [16]. The SPR of Zn doped Ag NPs influences the performance of Ag NPs in different reactions [17]. Moreover, Zn doping causes chemical alterations on the surface of nanoparticles [18]. The formation of the catalytic active sites on the surface of nanoparticles could be promoted by the introduction of Zn atom which can interfere with the reaction mechanisms and increase the rate of the reaction and optimize selectivity [19]. This synergistic effect between silver and zinc leads to improved performance in the catalytic degradation of pollutants, making Ag-Zn nanoparticles a superior choice for water treatment applications. Catalytic activity can be increased with optimal Zn doping ratios, while excessive doping can cause a decrease in the activity [20]. Activity loss with the excessive doping can be explained by three main factors. The first reason is that excessive Zn doping can distort SPR [21]. The second reason is that excessive amounts of Zn can cause the inappropriate location of the formation of critical chemical sites involved in catalytic reactions or cause agglomeration which decreases the chemically active sites [22, 23]. Finally, controlling electron and hole recombination may become challenging because of excessive Zn doping [24,25]. Consequently, to enhance the Ag NPs' catalytic performance, the doping ratio must be carefully adjusted [26].

Catalytic degradation using plants offers an ecological solution to environmental challenges. Green synthesis of nanoparticles using plant extracts has gained popularity as an environmentally friendly and sustainable method compared to conventional chemical and physical synthesis techniques

[27]. While chemical reduction methods are effective, they often contain dangerous chemicals and can produce toxic byproducts, which pose significant environmental and health risks [28]. Physical methods such as high-energy ball milling and laser ablation, on the other hand, are energy-intensive and require sophisticated equipment [29]. In contrast, green synthesis methods using biological materials are advantageous due to their simplicity, cost effectiveness and low environmental impact [30]. This biogenic approach not only reduces toxicity, but also utilizes the natural abundance and diversity of plant resources to produce nanoparticles with unique properties [31]. The effectiveness of plant extracts in NP syntheses arise from extract's contents such as polyphenols, ascorbic acids, carboxylic acids, terpenoids, amides, flavones which are responsible for reducing metal ions to form nanoparticles and stabilizing the nanoparticle cores and preventing agglomeration [32, 33]. *Polygonum cognatum* extract is preferred in this study for its richness in phytochemicals, particularly polyphenols and flavonoids providing a controlled synthesis of nanoparticles [34].

Polygonum cognatum is a medicinal and aromatic perennial plant, known as 'Madımak' in Turkey [35]. All anatomical parts of the plant have been used for treatments of several diseases as antioxidant, antimicrobial and antidiabetic medicine thanks to its high phenolic compounds, vitamin, mineral and flavonoid contents [34-37]. *Polygonum cognatum* has gained attention in scientific research for its potential medicinal and culinary uses in green synthesis processes. The findings of the antimicrobial activity of the plant extract have displayed a higher effectivity against a broad spectrum of bacteria and fungi [36, 38]. Moreover, the antiproliferative properties of *Polygonum cognatum* against some cancer types were also reported in literature [35, 37, 39].

Green synthesized nanoparticles have improved biocompatibility and reduced toxicity, making them suitable for various environmental and biomedical applications [40]. Some kinds of green synthesized nanoparticles by using different kinds of extracts are extensively used for the degradation of lethal and pestilential dyes [41, 42]. Among them, silver, zinc oxide, gold, iron oxide, palladium NPs are concluded to be most promising and efficient decolorization catalyst against a wide range of dyes including MO, MB reported in literature [41- 46]. However, nanoparticles synthesized using *Polygonum cognatum* extract has not been used in MO and MB catalytic degradation reaction studies before.

In this study, we present the green synthesis of non-doped and Zn-doped Ag NPs using *Polygonum cognatum* extract and investigate their catalytic performance in the degradation of water pollutants, MO and MB. The methodology and synthesis method adopted for different types of NPs using *Polygonum cognatum* extract has been limitedly studied in the literature [47-53]. To the best of our knowledge, Zn doped Ag NPs were synthesized and stabilized using *Polygonum cognatum* extract for the first time. The originality of this study lies both in the novel combination of silver and zinc in a green synthesis method with *Polygonum cognatum* extract and the fact that it has not been previously experienced in environmental treatment field presenting the research a unique perspective. The successfully synthesized nanoparticles were characterized using advanced analytical techniques, including STEM, EDS, XRF, XRD, FTIR, and ICP-MS. The catalytic activities of the obtained NPs as catalysts were evaluated using MO and MB degradation reactions. The reaction progressions were monitored using UV-Vis spectroscopy to determine turnover frequency (TOF) values and apparent rate constants (k_{app}). The results revealed that 9.0% Zn-doped Ag NPs exhibited significantly higher activity compared to bare Ag and 1.6% Zn-doped Ag NPs. 9.0% Zn-doped Ag NPs degraded 96.56% of MO in 15 minutes with a k_{app} of 0.2199 min^{-1} and a TOF of $1.65 \times 10^{-3} \text{ mol.g}^{-1} \text{ min}^{-1}$. Additionally, 9.0% Zn-doped Ag NPs degrade 98.38% of MB in 10 minutes with a k_{app} of 0.4445 min^{-1} and a TOF of $2.54 \times 10^{-3} \text{ mol.g}^{-1} \text{ min}^{-1}$. According to the results, Zn doped Ag NPs offer enhanced catalytic effects for the degradation of pollutants, emerging as promising agents for this purpose.

MATERIALS AND METHODS

Materials

The chemicals and materials used in this study were of high purity and commercially obtained. Zinc acetate dihydrate ($\text{Zn}(\text{Ac})_2$), Silver Nitrate (AgNO_3), Methyl Orange (MO), Methylene Blue (MB) and sodium borohydride (NaBH_4) were purchased from Sigma-Aldrich. These chemicals and solvents were used directly without any further purification.

Preparation of *Polygonum cognatum* Extract

Polygonum cognatum plant was collected from Sivas, Turkey and dried at ambient conditions. The dried plant was grounded into fine pieces and weighed as 10 mg. The powdered plant was dispersed in 100 mL distilled water and heated at 80 °C for 1 hour. The resulting extract was filtered using Whatman no: 1 filter paper to separate it from the pulp. Then, it was centrifuged at 9000 rpm and the supernatant-containing extract was kept at +4 °C to be used in nanoparticle synthesis and characterization processes.

Syntheses of Ag and Zn doped Ag Nanoparticles

In this study, AgNO_3 and $\text{Zn}(\text{Ac})_2$ were used as metal precursors in the synthesis of silver (Ag) and zinc-doped silver (Zn doped Ag) nanoparticles. Silver nanoparticles were first synthesized by using *Polygonum cognatum* extract according to the traditional green synthesis method in literature with some modifications such as pH, metal concentration and metal:extract volume ratio [54, 55]. These parameters were optimized by observing the agglomeration and stability of the NP suspension [56]. In a typical synthesis of Ag nanoparticles, 1 mL of extract was added to 9 mL of 6 mM AgNO_3 aqueous solution. The pH of the mixture was adjusted to 9 and color change was observed indicating the formation of Ag nanoparticles. The reaction mixture was left to stir for 2 hours for the complete formation of nanoparticles.

In the Zn doping method, core Ag nanoparticles were first synthesized, and these Ag nanoparticles acted as seeds for the nucleation of zinc nanoparticles on their surface [57]. It is generally proposed that Zn ions are reduced by components of extract, therefore zinc atoms are supposed to initially obtained in their metallic form on the surface of the Ag nanoparticles [58]. However, it would readily oxidize to ZnO under the reaction conditions. This is due to the dissolved oxygen in the reaction environment and the basic pH adjustments, which promote oxidation [59-61]. Likewise, for the synthesis of Ag nanoparticles to be acted as seeds for Zn; 1 mL of extract was added to 9 mL of 20 mM AgNO_3 aqueous solution [57]. The pH of the mixture was adjusted to 9 and left to stir for 2 hours. Then, 0.5 mL of 10 mM $\text{Zn}(\text{Ac})_2$ aqueous solution was added to the Ag NP suspension. It is well known for the zinc nanoparticle formation that the average size decreases with increased pH [62, 63]. Therefore, pH of the mixture was brought to 10 and the mixture was left to stir for another hour. At the end of the reaction, the pH of the solutions was fixed at 7. The second synthesis for Zn doping was carried out again under the same conditions by increasing the Zn amount to 3 mL. All the nanoparticle suspensions were centrifuged at 9000 rpm to separate the agglomerated parts, and the dispersed nanoparticles remaining in the supernatant were stored at 4 °C for characterization and evaluation of their catalytic activities.

Characterization Studies

Nanoparticle size and morphology were displayed through Scanning Transmission Electron Microscopy (STEM, ZEISS Gemini SEM 500) using 5 μL of NP suspension by dropping and drying it on carbon-coated Cu grids. Elemental content of NP suspensions was identified by Energy Dispersive X-ray Spectroscopy (EDS) analysis (SEM, ZEISS Gemini SEM 500) by coating 10 μL of sample with a 4.30 nm thick layer of iridium on a carbon band. The elemental analysis was also achieved through

energy dispersive X-ray fluorescence (EDXRF, Rigaku NEX CG) spectrometry. The measurement conditions were 50 kV, 2.00 mA, helium atmosphere, and 300 s of measurement time with a 50 kV-50W end-window palladium-anode X-ray tube. The crystalline structure of NPs was investigated using X-ray Diffraction measurement (XRD, PANalytical EMPYREAN) with Cu K α radiation for 2 θ values between 10 $^{\circ}$ -90 $^{\circ}$. The structural analysis of the extract and NPs synthesized with the same extract were carried out using Fourier Transform Infrared Spectroscopy (FTIR, Thermo Scientific-Nicolet IS20) to observe the functional groups of the samples. The quantitative analysis of Ag and Zn elements existing in NP suspension was achieved using inductively coupled plasma mass spectrometry (ICPMS, Agilent Technologies 7900) by dissolving samples in conc. HCl prior to the analysis.

Catalytic Studies

The catalytic activity of the biosynthesized Zn doped Ag NP was assessed against MO and MB using NaBH $_4$ as reducing agent. The catalytic tests were carried out by mixing aqueous solution of NaBH $_4$ (100 μ L, 0.1 M) and MO (2 mL, 5 mg/mL) or MB (2 mL, 5 mg/mL) with varying amounts of NP suspensions (400, 600, 800, 900 μ L) in 3 mL cuvette against constant Ag concentration (1400 ppm) for all type of NPs (bare Ag NP, 1.6% Zn doped Ag NP, 9.0% Zn doped Ag NP). The reaction progressions were followed with UV-Vis spectroscopy. The absorption spectra were recorded at RT.

The rate constants of the reduction reactions were determined by measuring the decrease in the absorbance of the MO and MB over time. In the degradation studies of MO and MB, NaBH $_4$ was employed at significantly high concentrations to achieve pseudo-first-order reaction conditions. Under these circumstances, the concentration of NaBH $_4$ remains substantially constant throughout the reaction, allowing the reaction kinetics to be simplified and treated as first-order with respect to the dye (MO or MB) alone. The apparent rate constant (kapp) was determined by plotting ln(C/C $_0$) versus time, where C is the concentration of the dye at a given time and C $_0$ is the initial concentration. The slope of this linear plot corresponds to the apparent rate constant, kapp, under the specified experimental conditions [64].

The turnover frequency (TOF) is another important parameter for determining the activities of catalysts and defined as moles of degraded dye per gram of catalyst per minute as given in equation (1), was further used for the catalyst activity evaluation [65, 66].

$$TOF = \frac{\text{mole of dye}}{\text{g catalyst}} \times \frac{1}{\text{min}} \quad (1)$$

RESULTS AND DISCUSSION

Nanoparticle Characterization

Polygonum cognatum extract was used as a reductant and stabilizer for the green synthesis of non-doped Ag NPs and Zn-doped Ag NPs. After the optimized synthesis of NPs, the reaction mixture immediately turned into a dark brown color, indicating the formation of NPs. The NPs were then characterized using the following microscopic and spectroscopic techniques.

The Ag concentration in NP suspensions were determined from ICP-MS measurements. The catalyst and Zn amounts were estimated from Ag concentrations in NP suspensions and the results are given in Table 1 and 2. The catalytic reduction of MO and MB was monitored spectrophotometrically using a UV-Vis Spectrophotometer (Agilent Technologies Cary 60) at intervals of 1 or 5 minutes at room temperature.

STEM images and EDS analysis of non-doped and Zn-doped Ag NPs were investigated. Figure 1a shows the STEM image of non-doped Ag NPs and in Figure 1b, the EDS spectrum of the same sample is presented, and the presence of Ag elements is clearly detected. Figure 1c shows the STEM

image of NPs with 1.6 % Zn doping and in Figure 1d, the EDS spectrum of the same sample is presented, and the presence of Ag and Zn elements is clearly detected.

Table 1

Ag and Zn amounts (ppm) estimated from ICP-MS measurement in NP suspensions.

	Ag, ppm	Zn, ppm
Ag NP	1875.1	-
1.6 % (w/w) Zn doped Ag NP	1832.3	30.0
9.0 % (w/w) Zn doped Ag NP	1478.9	146.3

Table 2

Zn and catalyst amounts (mg) in 0.8 mL NP suspension with constant Ag concentration (1400 ppm Ag)

	Ag, ppm	Zn, ppm	Catalyst, mg
Ag NP	1.12	-	1.12
1.6 % (w/w) Zn doped Ag NP	1.12	0.017	1.137
9.0 % (w/w) Zn doped Ag NP	1.12	0.11	1.23

Similarly, the STEM image (Figure 1e) and EDS spectrum (Figure 1f) of Ag NPs with 9.0% Zn doping were also analyzed. The EDS spectra clearly reveal the presence of Ag and Zn and obvious increase in the Zn amount. According to the STEM images, both NPs synthesized through the green method are of spherical shapes. It was observed that with increasing Zn doping, the NPs had homogeneous size distribution with a ~15 nm particle size, low agglomeration, and enhanced stability in aqueous medium for 9.0% Zn doping.

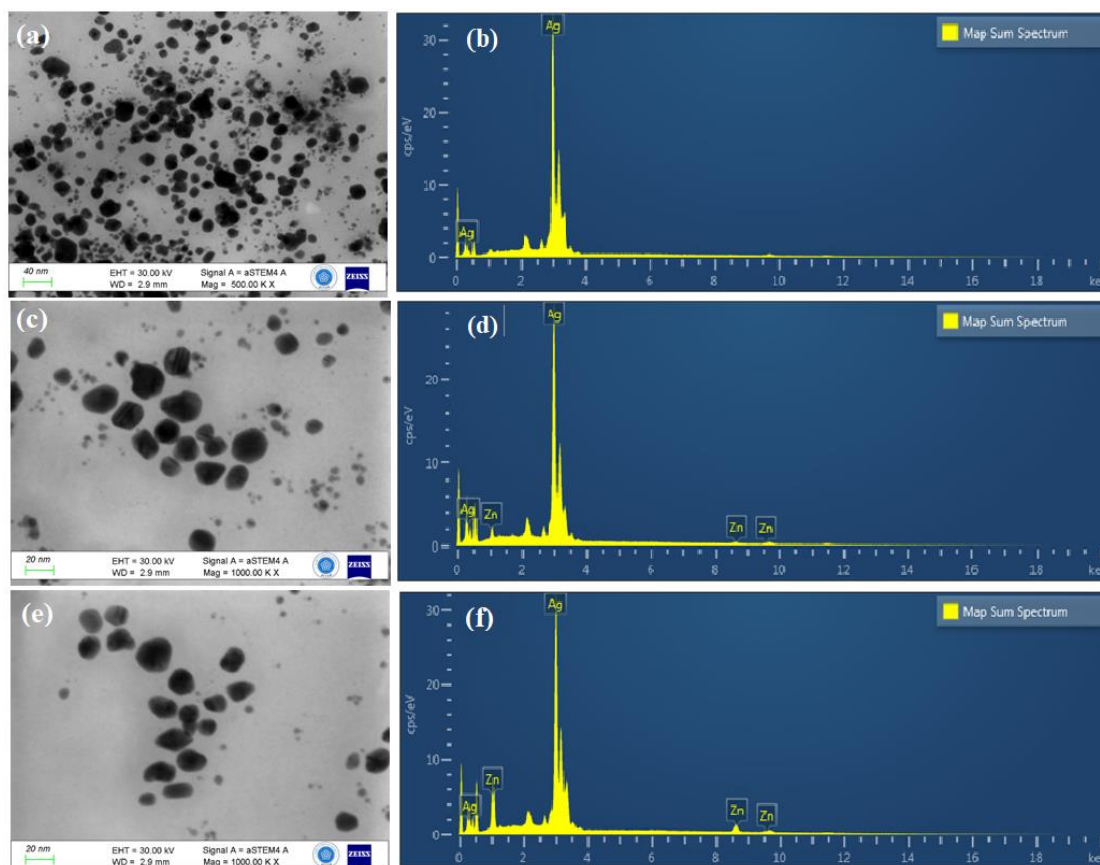


Figure 1

STEM image and its corresponding EDS spectra of Ag NPs (a-b), 1.6 % Zn Doped Ag NPs (c-d), 9.0 % Zn Doped Ag NPs (e-f)

In X-ray fluorescence (XRF) analysis, characteristic prominent peaks for each NP spectrum were observed at energy levels consistent with the elemental composition of the NPs, as seen in Figure 2. Additional peaks corresponding to Zn emerged in the spectrum, indicating the successful incorporation of Zn into the NP structure. Moreover, a proportional increase in the Zn-K α peak intensity was observed with the increased Zn doping ratio from 1.6% to 9.0% since Zn incorporation into the lattice sites of Ag NPs alters the crystal structure and electronic configuration of the NPs, leading to a more pronounced emission of characteristic X-rays.

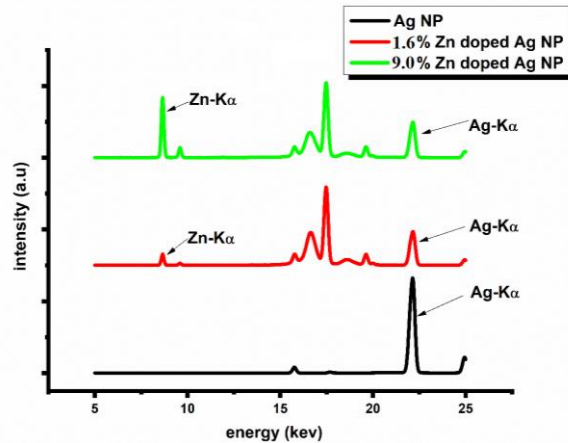


Figure 2
XRF spectra of Ag NPs, 1.6 % Zn doped Ag NPs and 9.0 % Zn doped Ag NPs

The X-ray diffraction (XRD) spectra presented in the Figure 3 depict the crystalline structure of Ag NPs, as well as Ag NPs doped with 9.0% Zn. For the Ag nanoparticles, the peaks are observed at approximately 38°, 44°, 64°, 77°, and 81°, corresponding to the (111), (200), (220), (311) and (222) crystallographic planes, respectively [52, 67-69]. The pure Ag NPs exhibit a crystal structure consistent with face-centered cubic (fcc) silver (JCPDS 87-0720) [69]. The Zn doped Ag NP spectrum presents both Zn and Ag peaks, despite small deviations for Ag peaks indicating that Zn doping occurred only at surface level and did not affect the crystalline structure of both species [70]. The peaks belonging ZnO are located at around 32°, 34°, 48°, 55°, 62°, 72° correspond to the (100), (002), (102), (110), (112) and (201) planes, respectively [71-73]. Sample reveals that the Zn-doped Ag NPs contain a phase corresponding to wurtzite ZnO (JCPDS 36-1451), indicating the successful doping of Ag NPs with Zn [74]. Unidentified peaks below 2 θ values of 30° are likely attributed to the extract [75].

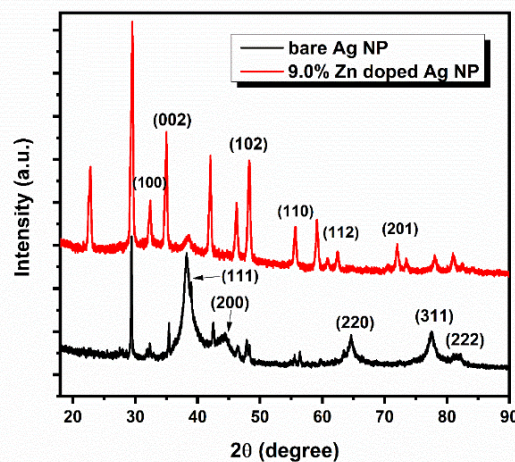


Figure 3
XRD spectra of Ag nanoparticles and 9.0% Zn doped Ag nanoparticles

FTIR analysis reveals similar spectral characteristics for the synthesized non-doped and Zn doped Ag NPs compared to the plant extract (Figure 4). In the FTIR spectrums, there are four peaks at similar positions with slight shifts in peak frequencies since the present functional groups of the extract are responsible for the reduction and capping of NPs proving the synthesis of NPs from the extract. The prominent peaks of extract are observed at 3253 cm^{-1} , 2921.08 cm^{-1} , 1598.53 cm^{-1} , 1293.99 cm^{-1} , indicating O-H stretching of phenolic groups [76], aliphatic C-H stretching vibrations [77], C=C stretching from aromatic rings [50], C-N vibrations [78], respectively. Ag generally absorbs very poorly in the infrared region and Ag-Ag metallic bond vibrations establish below 400 cm^{-1} [79]. Therefore, a distinct absorption band for Ag could not be seen in regions between ($4000\text{-}400\text{ cm}^{-1}$). Moreover, the amount of Zn in NP composition is as maximum %9 and the presence of the absorption bands of functional groups of the plant extract may mask some of the weak and unclear bands of metal nanoparticles in the FTIR spectrum [70]. Likewise, a distinct absorption band for Zn could not be observed in the spectrum, too. However, an additional peak at 2363.40 cm^{-1} and 2335.88 cm^{-1} as distinct from that of the extract is expected from vibration of the C=O bond of the CO_2 molecule that is chemisorbed during drying of NP surfaces [80, 81]. Additionally, the peak at 808.10 cm^{-1} observed in both NPs' spectrum distinct from that of the extract arises from the adsorption of residual NO_3^- groups to the extract components [82, 83].

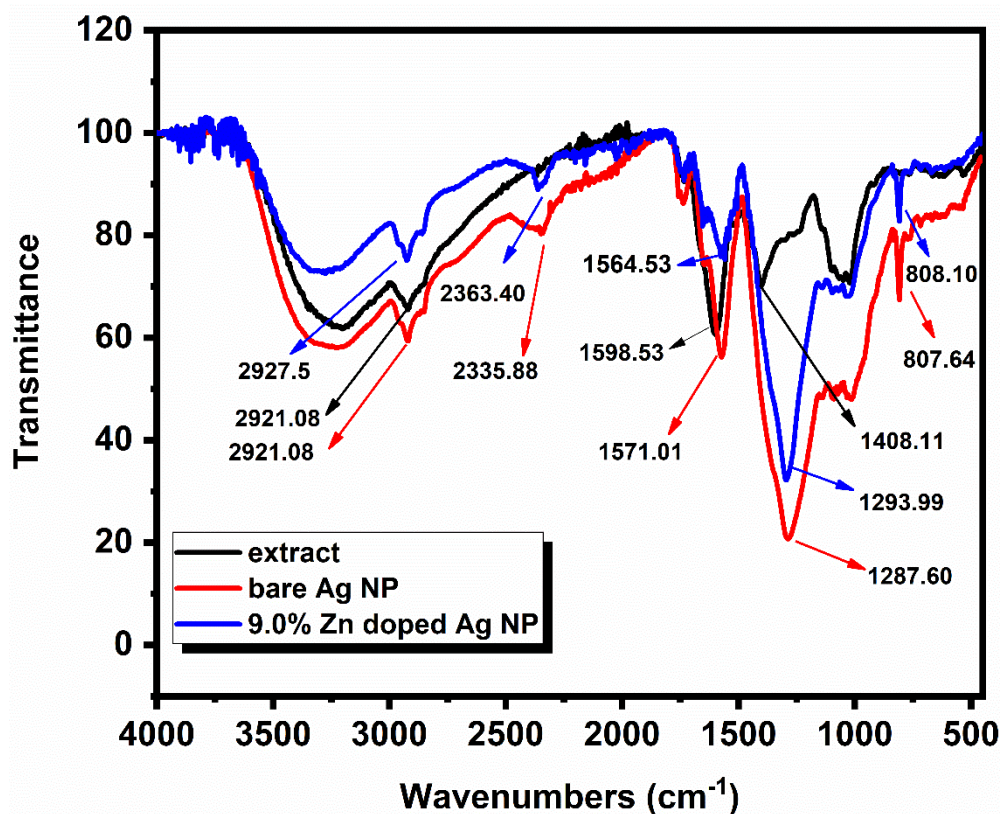


Figure 4
FTIR spectra of extract, Ag NPs, and 9.0% Zn doped Ag nanoparticles

Results of the Catalytic Studies

The degradation of MO and MB using Zn-doped Ag nanoparticles was carefully monitored by UV-Vis spectroscopy in the range 380-600 nm for 30 minutes. This method is a powerful tool to understand the evolution of the catalytic degradation process over time and to evaluate the efficiency of the nanomaterial. For monitoring the catalytic degradation of Methyl Orange by UV-Vis spectroscopy, the most prominent characteristic absorption peak which is around 464 nm is usually followed. When using UV-Vis spectroscopy to monitor the catalytic degradation of Methylene Blue, characteristic

absorption peaks at 664 nm are usually observed with time.

As can be seen from the UV-Vis absorption spectra in Figure 5a and Figure 6a, in the presence of bare Ag NPs, the reaction did not significantly progress, indicating that Ag NPs have a limited propensity to catalyze the degradation of MO and MB. In contrast, when Ag NPs were doped with Zn, the increase in activities was observed (Figure 5b, 5c and Figure 6b, 6c). Moreover, as the amount of Zn doping increased, the degradation of MO and MB increased while the degradation times decreased (Figure 5d and Figure 6d), indicating an acceleration of the reaction rate (Table 3).

The catalytic activity of bare Ag NPs can be considered very low because the percent degradation of MO and MB are 24.01 and 37.63, respectively at the end of the 30 min when the bare Ag NPs are used as the catalyst. On the other hand, when the 1.6 % Zn doped Ag NP was used as the catalyst, percent conversion was increased to 46.87 for MO degradation and the required time for the conversion decrease to 25 min (Figure 5b and Table 3). While the Zn doping amount was increased from 1.6 to 9.0 % methyl orange degradation also increased to 96.56% and the required time decreased to 15 min (Figure 5c).

As shown in Fig. 5c, nearly the complete degradation of MO could be observed in 15 min. Based on the linear relationship between $\ln(C/C_0)$ and reaction time (Figure 7a), the apparent rate constant (k_{app}) was calculated as 0.2199 min^{-1} for the 9.0% Zn doped Ag NP catalyzed MO degradation. The rate of the reaction was increased nearly 10-fold with the increase of Zn doping. (Figure 7a and Table 3). The TOF value of the 9.0% Zn doped Ag NP was determined as $1.65 \times 10^{-3} \text{ mol.g}^{-1} \text{ min}^{-1}$.

Similarly, the toxic MB dye can be degraded quickly in the presence of Zn doped Ag NPs as evidenced by the rapid disappearance of characteristic absorption peak of MB at 664 nm in 10 min (Fig. 6c), suggesting its high catalytic activity. When the spectra obtained for MB degradation were analyzed, it was found that the degradation of methylene blue increased from 78.36 % to 98.38 % when the doping amount was increased from 1.6% to 9.0% (Figure 6b and c). Further calculation based on the linear relationship between $\ln(C/C_0)$ and reaction time yielded an apparent rate constant of 0.4445 min^{-1} for the reduction reaction of MB catalyzed by the 9.0 % Zn doped Ag NP (Figure 7b). The TOF value of the 9.0% Zn doped Ag NP was determined as $2.54 \times 10^{-3} \text{ mol.g}^{-1} \text{ min}^{-1}$ and increased nearly 3 fold according to 1.6% Zn doped Ag NP ($0.9 \times 10^{-3} \text{ mol.g}^{-1} \text{ min}^{-1}$) suggesting the activity toward degradation of MB increase when Zn doping increased. When comparing both the apparent rate and TOF results, it can be said that 9.0% Zn-doped Ag NPs can be used as a more active catalyst for MB degradation compared to MO degradation.

With increasing Zn doping, the catalytic activity of the nanoparticles increased in the degradation reactions of both toxic dyes. (Table 3). The increased activity can be attributed to some factors. Firstly, Zn doping alters the surface properties of Ag NPs, leading to changes in their catalytic behavior. This modification can enhance the interaction between the catalyst and the reactants, thereby improving the catalytic activity [66]. Secondly, Zn doping can create additional active sites on the surface of Ag NPs, which are facilitate to catalytic reactions. These new active sites may facilitate the adsorption and activation of reactant molecules, promoting faster reaction rates [65]. Finally, the combination of Ag and Zn in doped nanoparticles can result in synergistic effects, where the presence of Zn enhances the catalytic properties of Ag. This synergistic interaction between Ag and Zn can lead to improved catalytic performance compared to pure Ag nanoparticles [84].

Table 3
Comparison of the rate constant and TOF for the catalytic reduction of MO and MB

Dye	Catalyst	Catalyst amount for 0,8 mL (mg)	% Degradation	Time (min)	Rate constant, k_{app} (min^{-1})	TOF $\times 10^{-3}$, ($\text{mol.g}^{-1} \text{min}^{-1}$)
Methyl Orange	Ag NP	1.12	24.01	30	0.0106	0.91
	1.6% Zn doped Ag NP	1.137	46.87	25	0.0239	1.10
	9.0% Zn doped Ag NP	1.23	96.56	15	0.2199	1.65
Methylene Blue	Ag NP	1.12	37.63	35	0.0171	0.79
	1.6% Zn doped Ag NP	1.137	78.36	30	0.0678	0.9
	9.0% Zn doped Ag NP	1.23	98.38	10	0.4445	2.54

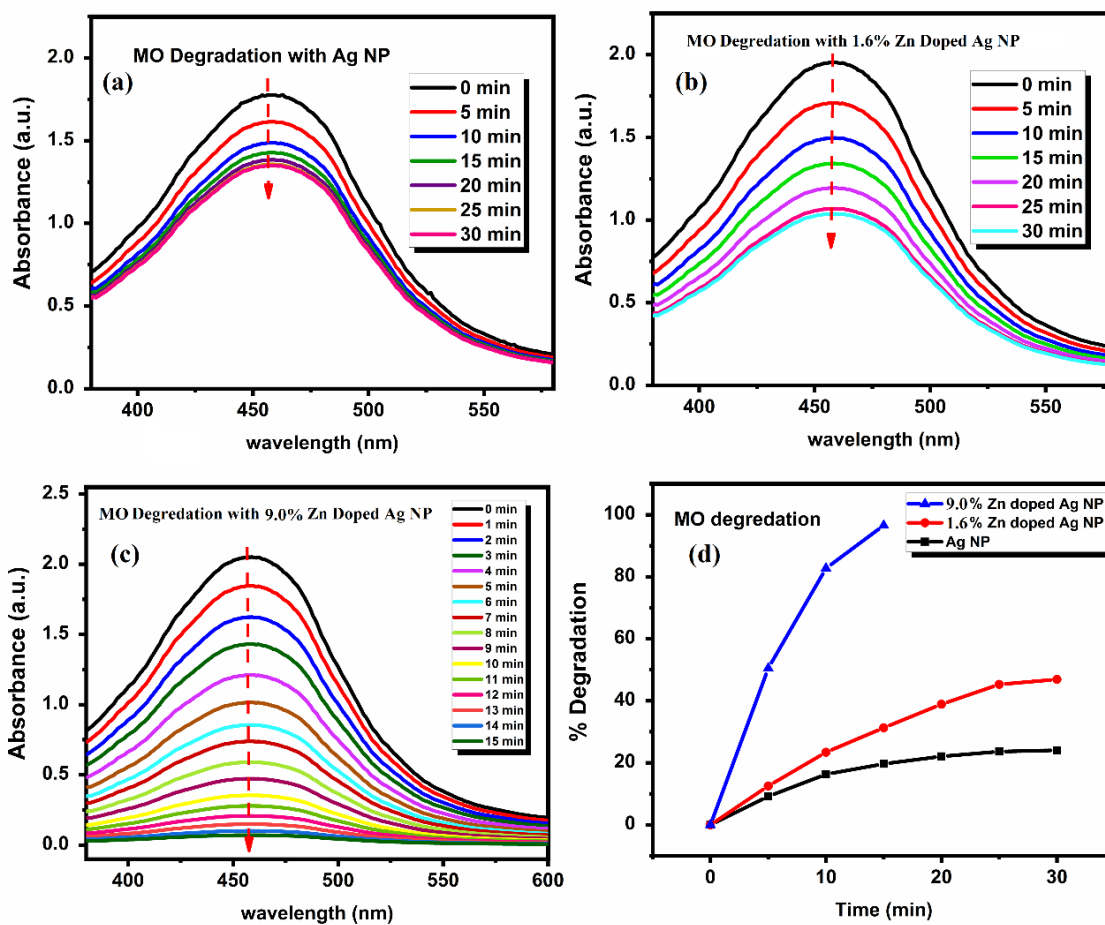


Figure 5
The UV-Vis absorption spectra of MO dye degradation using a) Ag NP, b) 1.6% Zn doped Ag NP, c) 9.0% Zn doped Ag NP and d) degradation percents of MO vs time for three catalysts

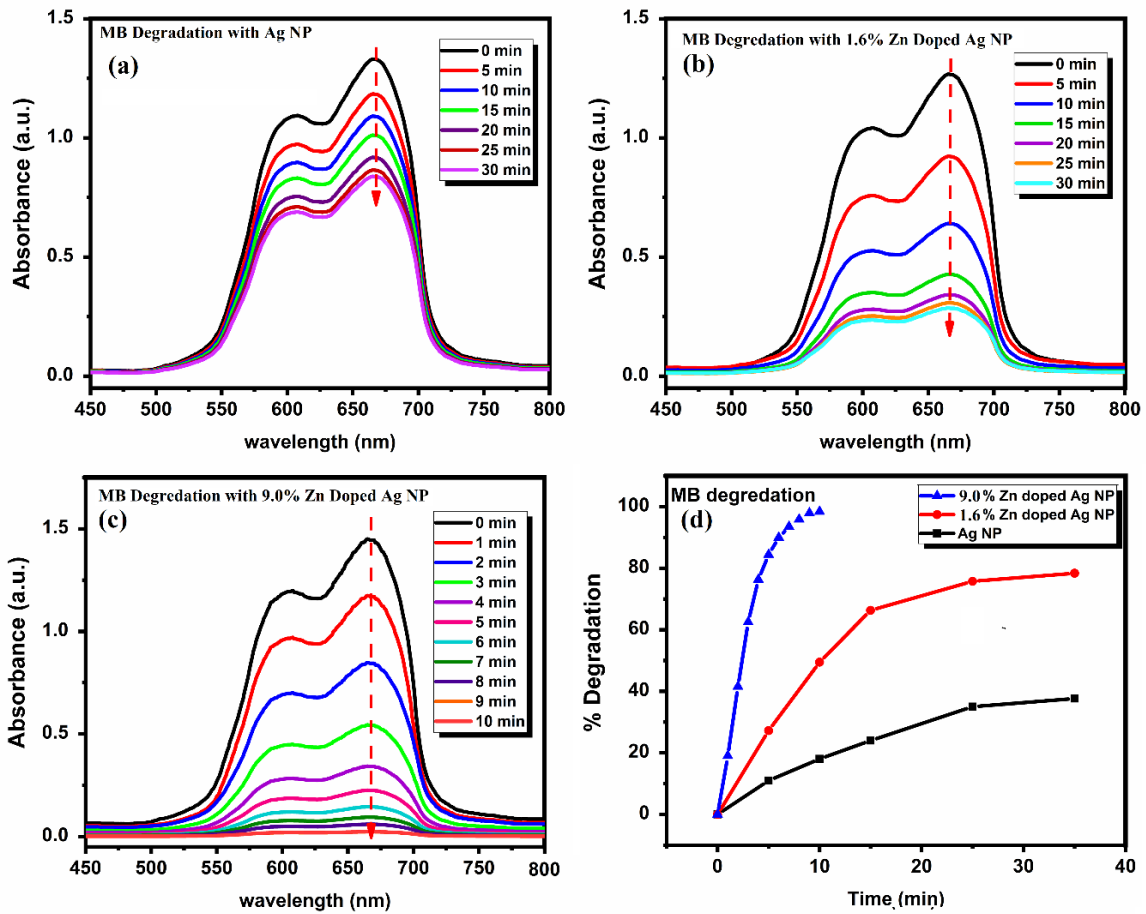


Figure 6

The UV-Vis absorption spectra of MB dye degradation using a) Ag NP, b) 1.6% Zn doped Ag NP, c) 9.0% Zn doped Ag NP and d) degradation percents of MB vs time for three catalysts

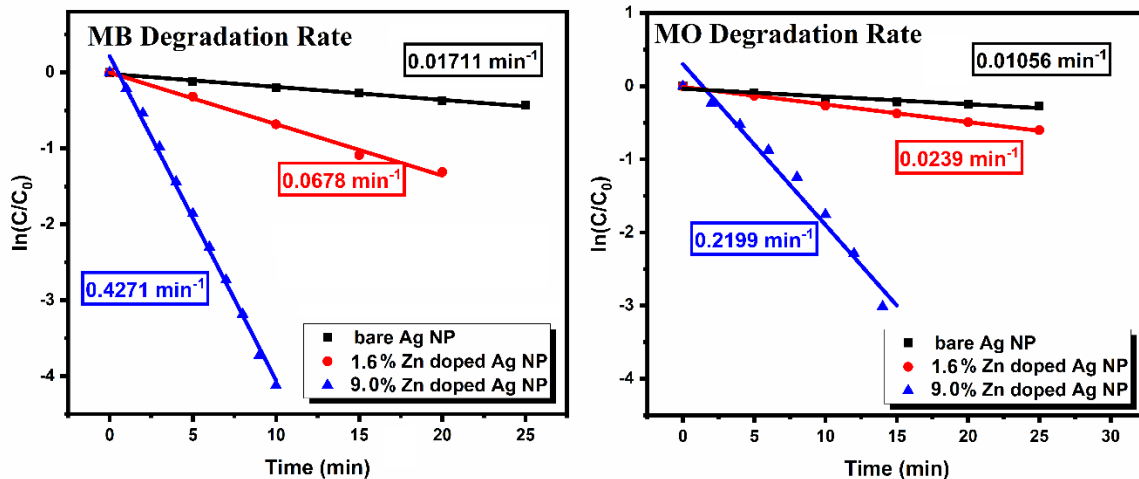


Figure 7

Plot of $\ln(C/C_0)$ versus time (min) for the degradation of a. MO b. MB using Ag NP, 1.6% Zn doped Ag NP, and 9.0% Zn doped Ag NP.

After determining the activity of 9.0% Zn doped Ag NP, loading density studies were conducted. The amounts of dyes added to the reaction medium and the used amount of NaBH_4 were kept constant, and the amounts of 9.0% Zn doped Ag NP catalyst added to the reaction environment were changed.

0.4, 0.6, 0.8-, and 0.9-mL NP suspensions were separately added to the reaction environments, and percentage degradations were monitored. When 0.9 mL NP suspension was added to reaction instead of 0.8 mL than the percent degradation increases only from 96.56% to 97.02% for MO and from 98.38% to 98.76% for MB. (Table 4) As a result of the studies, it was found that adding 0.8 mL NP suspension yielded optimal results and increasing the added NP amount beyond 0.8 mL did not result in a significant change in the percent degradation of the two dyes. This could be attributed to the saturation of reactants on the catalyst's available surface, where increasing the amount of catalyst did not increase the percent degradation at the same reaction time [85].

Table 4

MO and MB degradation values with the change of 9.0% Zn doped Ag NP catalyst amount

Dye	NP suspension(mL)	% degradation	Time(min)
MO	0.4	87.21	30
	0.6	92.19	25
	0.8	96.56	15
	0.9	97.02	15
MB	0.4	89.49	30
	0.6	91.69	25
	0.8	98.38	10
	0.9	98.76	10

Catalytic degradations of MO and MB in the presence of constant catalyst and NaBH₄ amount were also evaluated to examine the impact of the dye concentration on the catalytic reaction process. The concentrations of the dyes were changed from 2.5 mg/mL to 7.5 mg/mL while maintaining the 9.0% Zn doped Ag NP catalyst loading (0.8 mL) and NaBH₄ concentration (0.1 M) The variation of the percent degradation of dyes at the same time interval was presented in Table 5. It is observed that with the rise of dye concentration the value of percent degradation increased up to a 5 mg/mL concentration after that it decreased with the rise of dye concentration to 7.5 mg/mL. MO degradation firstly increase from 96.09 to 96.56 with the increase of dye concentration from 2.5 to 5 mg/mL. However, when the concentration was increased to 7.5 mg/mL degradation decrease to 90.93%. Similarly, MB degradation first increase from 92.71 to 98.38 with the increase of dye concentration from 2.5 to 5 mg/mL. However, degradation decrease to 97.07% with the increase in the concentration. In the low concentrations of the dyes, the percent degradations were found as low value because most of the catalytic sites were occupied by the borohydride ions. With the increase in the concentrations of dyes, they began to dominate most of the catalytic surface, resulting in the increase in the percent degradation. However, at higher concentrations, a significant portion of the catalytic surface became occupied by the dye molecules due to their high binding capability. This hindered the reaction with BH₄⁻ ions, consequently reducing the percent degradation values [86].

Table 5

MO and MB degradation with 9.0% Zn doped Ag NP

	Dye amount (mg/mL)	% Degradation	Time(min)
MO	2.5	96.09	30
	5	96.56	15
	7.5	90.93	15
MB	2.5	92.71	30
	5	98.38	10
	7.5	97.07	10

Table 6

Some studies from literature for methylene blue and methyl orange dyes degradation by various biosynthesized Ag nanoparticles with the use of NaBH_4 .

Nanomaterial	Biosynthesis source	Dye degraded	Time for degradation	Degradation %	Ref.
9.0% Zn doped Ag NP	<i>Polygonum cognatum</i>	Methylene blue	10	98.38	This work
Ag	<i>Lathyrus brachypterus</i>	Methylene blue	6	98	[87]
Ag	<i>Albizia procera</i>	Methylene blue	70	99.6	[88]
Ag	<i>Gmelina arborea</i>	Methylene blue	7	100	[89]
Ag	<i>C. paradisi</i> (Paradise citrus)	Methylene blue	4	93.29	[90]
Ag	<i>Blumea lacera</i>	Methylene blue	24	56	[91]
Ag/ZnO nanocomposite	<i>Valeriana officinalis</i>	Methylene blue	2	100	[92]
9.0% Zn doped Ag NP	<i>Polygonum cognatum</i>	Methyl orange	15	96.56	This work
Ag	<i>Heterotheca subaxillaris</i>	Methyl orange	11	100	[93]
Ag	<i>Cassia alata</i>	Methyl orange	120	98.6	[94]
Ag	<i>Clitoria ternatea</i>	Methyl orange	10	100	[95]
Ag	<i>Hibiscus tiliaceus</i>	Methyl orange	45	100	[96]
Ag	<i>S. costus</i>	Methyl orange	135	72.88	[97]
Ag/ZnO nanocomposite	<i>Valeriana officinalis</i>	Methyl orange	4	100	[92]

In recent studies on the degradation of methylene blue (MB) and methyl orange (MO) dyes using green synthesized Ag nanoparticles, a variety of biosynthesis sources and their effectiveness have been explored (Table 6). For instance, NP synthesized using *Lathyrus brachypterus* extract enabled 98% degradation of MB in just 6 minutes, while that of *Albizia procera* showed a 99.6% degradation of MB in 70 minutes. NP synthesized using *Gmelina arborea* demonstrated complete degradation (100%) of MB in 7 minutes. On the other hand, degradation of MO using Ag nanoparticles synthesized from sources like *Heterotheca subaxillaris* flower and *Cassia alata* resulted in 100% degradation in 11 and 120 minutes, respectively. When comparing these literature results to our findings using 9.0% Zn-doped Ag nanoparticles, it is evident that our method yields superior results. Our nanoparticles achieved 98.38% degradation of 5 mg/mL MB in just 10 minutes and 96.56% degradation of 5 mg/mL MO in 15 minutes. These results demonstrate that our Zn-doped Ag nanoparticles not only achieve high degradation percentages but also do so in significantly shorter times compared to many biosynthesized Ag nanoparticles reported in the literature. This highlights the potential of our Zn-doped Ag nanoparticles as a highly efficient alternative for dye degradation.

CONCLUSION

In this study, Ag NP and Zn doped Ag NP were successfully synthesized using *Polygonum cognatum* plant as reducing and stabilizing agent by systematically varying zinc doping ratio (bare Ag NP, 1.6% Zn-doped Ag NP, and 9.0% Zn-doped Ag NP). The catalytic activities of synthesized nanoparticles were studied using the MO and MB dyes degradation reactions using a solution of sodium borohydride (NaBH_4) as the reducing agent. Some characterization techniques such as STEM, EDS, XRF, XRD, FTIR and ICP-MS analyses verified the effective incorporation of Zn into the Ag NP matrix, demonstrating the presence of components and structural alterations in the 9.0% Zn doped Ag NPs. UV-Vis spectroscopy was used to observe the process of degradation.

In catalytic experiments, different concentrations of nanoparticle (NP) suspensions (400, 600,

800, and 900 μL) were added to 3 mL cuvettes while the Ag concentration remained constant (1400 ppm) for all types of NPs (bare Ag NP, 1.6% Zn-doped Ag NP, and 9.0% Zn-doped Ag NP). According to catalytic degradation experiments, Zn doping at 9.0% significantly improved the degradation efficiency compared to bare Ag NPs and 1.6% Zn-doped Ag NPs. Specifically, the 9.0% Zn-doped Ag NPs achieved 96.56% degradation of MO in 15 minutes and 98.38% degradation of MB in 10 minutes, with rate constants of 0.2199 min^{-1} and 0.4445 min^{-1} , respectively. Additionally, the turnover frequencies (TOF) for MO and MB were $1.65 \times 10^{-3} \text{ mol.g}^{-1} \text{ min}^{-1}$ and $2.54 \times 10^{-3} \text{ mol.g}^{-1} \text{ min}^{-1}$, respectively. Increasing the doping amount of Zn from 1.6% to 9.0% greatly decrease reaction times and improve degradation efficiency with MO degradation improving from 46.87% in 25 minutes ($k_{\text{app}} = 0.0239 \text{ min}^{-1}$, $\text{TOF} = 1.10 \times 10^{-3} \text{ mol.g}^{-1} \text{ min}^{-1}$) to 96.56% in 15 minutes, and MB degradation increasing from 78.36% in 30 minutes ($k_{\text{app}} = 0.0678 \text{ min}^{-1}$, $\text{TOF} = 0.9 \times 10^{-3} \text{ mol.g}^{-1} \text{ min}^{-1}$) to 98.38% in 10 minutes. The optimal NP suspension volume was found to be 0.8 mL, beyond which no significant improvement in degradation was observed. Furthermore, the study found that the optimal dye concentration for degradation was 5 mg/mL, as higher concentrations led to decreased efficiency due to surface saturation of the catalyst. These findings highlight the effectiveness of 9.0% Zn-doped Ag NPs as catalysts for the rapid and efficient degradation of hazardous dyes, presenting a viable solution for wastewater treatment applications.

Author Contributions

Research Design (CRediT 1) M.A. (40%) - T.N.A. (60%)

Data Collection (CRediT 2) M.A. (30%) - Ü.Ü. (20%) - T.N.A. (50%)

Research - Data Analysis - Validation (CRediT 3-4-6-11) M.A. (30%) - Ü.Ü. (20%) - T.N.A. (50%)

Writing the Article (CRediT 12-13) M.A. (50%) - T.N.A. (50%)

Revision and Improvement of the Text (CRediT 14) M.A. (40%) - Ü.Ü. (20%) - T.N.A. (40%)

Financing

Not applicable.

Data availability

The data presented in this study are available on request from the corresponding author.

Conflict of interest

The authors declare that there are no conflicts of interests.

REFERENCES

- [1] B. Akgayev, S. Akbayrak, M. Yılmaz, M.S. Büker, V. Unsur, Assessing the feasibility of photovoltaic systems in Türkiye: Technical and economic analysis of on-grid, off-grid, and utility-scale PV installations, *Necmettin Erbakan University Journal of Science and Engineering*. 6(1) (2024), 69-92. doi:10.47112/neufmbd.2024.33
- [2] M. Ismail, K. Akhtar, M.I. Khan, T. Kamal, M.A. Khan, M.A. Asiri, S.B. Khan, Pollution, toxicity and carcinogenicity of organic dyes and their catalytic bioremediation, *Current pharmaceutical design*. 25(34) (2019), 3645-3663. doi:10.2174/1381612825666191021142026
- [3] M.A. Al-Nuaim, A.A. Alwasiti, Z.Y. Shnain, The photocatalytic process in the treatment of polluted water, *Chemical papers*. 77(2) (2023), 677-701. doi:10.1007/s11696-022-02468-7
- [4] M. Priyadarshane, U. Mahto, S. Das, Mechanism of toxicity and adverse health effects of environmental pollutants, In *Microbial biodegradation and bioremediation*. (2022), 33-53. Elsevier. doi:10.1016/B978-0-323-85455-9.00024-2
- [5] S. Bulbul, E. Ayhan, H. Gökmeşe, Termik santral atığı olan kömür külünün SBR matrisli bileşiklere ilave edilmesinin mekanik özelliklere etkisi, *Necmettin Erbakan University Journal of Science and Engineering*. 5(2) (2023), 96-107. doi:10.47112/neufmbd.2023.14
- [6] M.A. Al-Nuaim, A.A. Alwasiti, Z.Y. Shnain, The photocatalytic process in the treatment of polluted water, *Chemical papers*, 77(2) (2023) 677-701. doi:10.1007/s11696-022-02468-7
- [7] A. Saravanan, P.S. Kumar, D.V.N. Vo, S. Jeevanantham, S. Karishma, P.R.A. Yaashikaa, review on catalytic-enzyme degradation of toxic environmental pollutants: Microbial enzymes, *Journal of Hazardous Materials*. 419 (2021), 126451. doi:10.1016/j.jhazmat.2021.126451
- [8] D. Astruc, Introduction: nanoparticles in catalysis, *Chemical reviews*. 120(2) (2020), 461-463. doi: 10.1021/acs.chemrev.8b00696
- [9] A. Dhaka, S.C. Mali, S. Sharma, R.A. Trivedi, review on biological synthesis of silver nanoparticles and their potential applications, *Results in Chemistry*. (2023), 101108. doi:10.1016/j.rechem.2023.101108
- [10] B. Mekuye, The Impact of size on the optical properties of silver nanoparticles based on dielectric function, *Nanotechnology and Nanomaterials Annual Volume* (2023). doi:10.5772/intechopen.113976
- [11] W. Lewandowski, M. Fruhnert, J. Mieczkowski, C. Rockstuhl, E. Górecka, Dynamically self-assembled silver nanoparticles as a thermally tunable metamaterial, *Nature communications*. 6(1) (2015), 6590. doi:10.1038/ncomms7590
- [12] G. Palani, H. Trilaksana, R.M. Sujatha, K. Kannan, S. Rajendran, K. Korniejenko, M. Uthayakumar, Silver nanoparticles for wastewater management, *Molecules*. 28(8) (2023), 3520. doi:10.3390/molecules28083520
- [13] M.A. Kareem, I.T. Bello, H.A. Shittu, P. Sivaprakash, O. Adedokun, S. Arumugam, Synthesis, characterization, and photocatalytic application of silver doped zinc oxide nanoparticles, *Cleaner Materials*. 3 (2022), 100041. doi:10.1016/j.clema.2022.100041
- [14] V. Vinitha, M. Preeyanghaa, V. Vinesh, R. Dhanalakshmi, B. Neppolian, V. Sivamurugan, Two is better than one: Catalytic, sensing and optical applications of doped zinc oxide nanostructures, *Emergent Materials*. 4 (2021), 1093-1124. doi:10.1007/s42247-021-00262-x
- [15] D. Ntemogiannis, M. Tsarmpopoulou, A. Stamatelatos, S. Grammatikopoulos, V. Karoutsos, D.I. Anyfantis, P. Pouloupoulos, ZnO Matrices as a platform for tunable localized surface plasmon resonances of silver nanoparticles, *Coatings*. 14(1) (2024), 69. doi:10.3390/coatings14010069
- [16] S. Lv, Y. Du, F. Wu, Y. Cai, T. Zhou, Review on LSPR assisted photocatalysis: effects of physical fields and opportunities in multifield decoupling, *Nanoscale Advances*. 4(12) (2022), 2608-2631. doi:10.1039/D2NA00140C

- [17] Y. Li, Q. Liao, W. Hou, L. Qin, Silver-based surface plasmon sensors: fabrication and applications, *International Journal of Molecular Sciences*. 24(4) (2023), 4142. doi:10.3390/ijms24044142
- [18] E. Vanags, I. Bite, L. Ignatane, R. Ignatans, A. Trausa, C.F. Tipaldi, K. Smits, Zinc Oxide Tetrapods Doped with Silver Nanoparticles as a Promising Substrate for the Detection of Biomolecules via Surface-Enhanced Raman Spectroscopy, *ChemEngineering*. 8(1) (2024), 19. doi:10.3390/chemengineering8010019
- [19] S. Raha, M. Ahmaruzzaman, ZnO nanostructured materials and their potential applications: progress, challenges, and perspectives, *Nanoscale Advances*. 4(8) (2022), 1868-1925. doi: 10.1039/D1NA00880C
- [20] H. Li, P. Wang, J. Qian, Y. Li, Q. Yuan, L. Du, Y. Chen, Zn-doped MnCe catalyst designed and applied for indoor low concentration formaldehyde removal and simultaneous antibacterial, *Materials Chemistry and Physics*. 305 (2023), 127946. 2023.127946. doi: 10.1016/j.matchemphys
- [21] Y. Sun, W. Zhang, Q. Li, H. Liu, X. Wang, Preparations and applications of zinc oxide based photocatalytic materials, *Advanced Sensor and Energy Materials*. (2023), 100069. doi:10.1016/j.asems.2023.100069
- [22] J. Schumann, M. Eichelbaum, T. Lunkenbein, N. Thomas, M.C. Alvarez Galvan, R. Schlögl, M. Behrens, Promoting strong metal support interaction: doping ZnO for enhanced activity of Cu/ZnO: M (M= Al, Ga, Mg) catalysts, *ACS catalysis*. 5(6) (2015), 3260-3270. doi:10.1021/acscatal.5b00188
- [23] M.L. Sun, Z.P. Hu, H.Y. Wang, Y.J. Suo, Z.Y. Yuan, Design strategies of stable catalysts for propane dehydrogenation to propylene, *ACS Catalysis*. 13(7) (2023), 4719-4741. doi:10.1021/acscatal.3c00103
- [24] N.A. Erfan, M.S. Mahmoud, H.Y. Kim, N.A. Barakat, Synergistic doping with Ag, CdO, and ZnO to overcome electron-hole recombination in TiO₂ photocatalysis for effective water photo splitting reaction, *Frontiers in Chemistry*. (2023), 11. doi:10.3389/fchem.2023.1301172
- [25] T. Mao, M. Liu, L. Lin, Y. Cheng, C.A Fang, study on doping and compound of zinc oxide photocatalysts, *Polymers*. 14(21) (2022), 4484. doi:10.3390/polym14214484
- [26] I.H. Ifijen, M. Maliki, B. Anegebe, Synthesis, photocatalytic degradation and antibacterial properties of selenium or silver doped zinc oxide nanoparticles: A detailed review, *OpenNano*. 8 (2022), 100082. doi: 10.1016/j.onano.2022.100082
- [27] D. Gupta, A. Boora, A Thakur, T.K. Gupta, Green and sustainable synthesis of nanomaterials: recent advancements and limitations, *Environmental Research*. 231 (2023), 116316. doi:10.1016/j.envres.2023.116316
- [28] P. Szczyglewska, A. Feliczak-Guzik, I. Nowak, Nanotechnology—general aspects: A chemical reduction approach to the synthesis of nanoparticles, *Molecules*. 28(13) (2023), 4932. doi:10.3390/molecules28134932
- [29] V. Harish, M.M. Ansari, D. Tewari, A.B. Yadav, N. Sharma, S. Bawarig, A. Barhoum, Cutting-edge advances in tailoring size, shape, and functionality of nanoparticles and nanostructures: A review, *Journal of the Taiwan Institute of Chemical Engineers*. 149 (2023), 105010. doi:10.1016/j.jtice.2023.105010
- [30] Y. T. Gebreslassie, F.G. Gebremeskel, Green and cost-effective biofabrication of copper oxide nanoparticles: Exploring antimicrobial and anticancer applications, *Biotechnology Reports*. (2024), e00828. doi:10.1016/j.btre.2024.
- [31] A.R. Bagheri, N. Aramesh, M.S. Hasnain, A.K. Nayak, R.S. Varma, Greener fabrication of metal nanoparticles using plant materials: A review, *Chemical Physics Impact*. 7 (2023), 100255. doi:10.1016/j.chphi.2023.100255

- [32] A.M.E. Shafey, Green synthesis of metal and metal oxide nanoparticles from plant leaf extracts and their applications: A review, *Green Processing and Synthesis*. 9(1) (2020), 304-339. doi:10.1515/gps-2020-0031
- [33] N.M. Ishak, S.K. Kamarudin, S.N. Timmiati, Green synthesis of metal and metal oxide nanoparticles via plant extracts: an overview, *Materials Research Express*. 6(11) (2019), 112004. doi:10.1088/2053-1591/ab4458
- [34] S. Gözcü, R.A. Uğan, H. Özbek, B. Gündoğdu, Z. Güvenalp, Evaluation of antidiabetic and antioxidant effects of *Polygonum cognatum* Meisn. and phytochemical analysis of effective extracts, *Biomedical Chromatography*. 38(3) (2024), e5809. doi:10.1002/bmc.5809
- [35] N. Eruygur, E. Ucar, M. Ataş, M. Ergul, M. Ergul, F. Sozmen, Determination of biological activity of *Tragopogon porrifolius* and *Polygonum cognatum* consumed intensively by people in Sivas, *Toxicology reports*. 7 (2020), 59-66. doi:10.1016/j.toxrep.2019.12.002
- [36] F. Demirgöl, M. Divriklioğlu-Kundak, O. Sağdıç, Bioactive properties, antibacterial activity, and color features of *Polygonum cognatum*: The effects of frozen storage and cooking process, *Food Science and Technology*. 42 (2022), e00322. doi:10.1590/fst.00322
- [37] R. Akpınar, G. Yıldırım Baştemur, B. Bıçak, N.O. Sanli, E. Mertoğlu Kamalı, M. Pekmez, S. Perçin Özkorucuklu, Phytochemical profiling, in vitro biological activities, and in silico (molecular docking and absorption, distribution, metabolism, excretion, toxicity) studies of *Polygonum cognatum* Meisn, *Journal of Separation Science*. 47(1) (2024), 2300750. doi:10.1002/jssc.202300750
- [38] A. Yıldırım, A. Mavi, A. Kara, Antioxidant and antimicrobial activities of *Polygonum cognatum* Meisn extracts, *Journal of the Science of Food and Agriculture*. 83(1) (2003), 64-69. doi:10.1002/jsfa.1288
- [39] M. Pehlivan, H.İ.K. Çöven, B. Çerçi, A. Eldem, T. Öz, N. Savlak, İ. Pirim, The cytotoxic effect of *Polygonum cognatum* and chemotherapeutic effect of doxorubicin on glioblastoma cells, *European Journal of Therapeutics*. 27(1) (2021), 50-54. doi:10.5152/eurjther.2021.20085
- [40] A.Q. Malik, T.U.G.,Mir, D. Kumar, I.A. Mir, A. Rashid, M. Ayoub, S. Shukla, A review on the green synthesis of nanoparticles, their biological applications, and photocatalytic efficiency against environmental toxins, *Environmental Science and Pollution Research*. 30(27) (2023), 69796-69823. doi:10.1007/s11356-023-27437-9
- [41] B. Mahesh, A comprehensive review on current trends in greener and sustainable synthesis of ferrite nanoparticles and their promising applications, *Results in Engineering*. (2023), 101702. doi:10.1016/j.rineng.2023.101702
- [42] A. Saravanan, P.S. Kumar, S. Karishma, D.V.N. Vo, S. Jeevanantham, P.R. Yaashikaa, C.S. George, A review on biosynthesis of metal nanoparticles and its environmental applications, *Chemosphere*. 264 (2021), 128580. doi:10.1016/j.chemosphere.2020.128580
- [43] B. Mahesh, A comprehensive review on current trends in greener and sustainable synthesis of ferrite nanoparticles and their promising applications, *Results in Engineering*. (2023), 101702. doi:10.1016/j.rineng.2023.101702
- [44] A.B. Daphedar, S. Kakkalameli, B. Faniband, M. Bilal, R.N. Bhargava, L.F.R. Ferreira, S. I. Mulla, Decolorization of various dyes by microorganisms and green-synthesized nanoparticles: current and future perspective, *Environmental Science and Pollution Research*. 30(60) (2023), 124638-124653. doi:10.1007/s11356-022-21196-9
- [45] S.S. Emmanuel, A.A. Adesibikan, O.D. Saliu, E.A. Opatola, Greenly biosynthesized bimetallic nanoparticles for ecofriendly degradation of notorious dye pollutants: A review, *Plant Nano Biology*. 3 (2023), 100024. doi:10.1016/j.plana.2023.100024
- [46] N.T. T. Nguyen, L.M. Nguyen, T.T.T. Nguyen, R.K. Liew, D.T.C. Nguyen, T. Van Tran, Recent advances on botanical biosynthesis of nanoparticles for catalytic, water treatment and agricultural

- applications: A review, *Science of the Total Environment*. 827 (2022), 154160. doi:10.1016/j.scitotenv.2022.154160
- [47] M. Yilmaz, A. Yilmaz, A. Karaman, F. Aysin, O. Aksakal, Monitoring Chemically and Green-Synthesized Silver nanoparticles in maize seedlings via Surface-Enhanced Raman Spectroscopy (SERS) and their phytotoxicity evaluation, *Talanta*. (225) (2021), 121952. doi:10.1016/j.talanta.2020.121952. doi:10.1016/j.talanta.2020.121952
- [48] Ö. Kaplan, N. Gökşen Tosun, Biosynthesis of iron, copper and silver nanoparticles using *Polygonum cognatum* and *tragopogon porrifolius* extracts and evaluation of their antimicrobial potentials, *Düzce Üniversitesi Bilim ve Teknoloji Dergisi*. 11(4) (2023), 2155–2167. doi:10.29130/dubited.1093468
- [49] N. Gürsoy, S. Elagöz, E. Gölge, *Polygonum cognatum* Meissn. ve funguslu ortamda sentezlenen gümüş nanopartiküllerinin (agnp) antimikrobiyal özelliklerinin araştırılması, *Türk Tarım ve Doğa Bilimleri Dergisi*. 7 (1) (2020), 221–230. doi: 10.30910/turkjans.680075
- [50] H. Meskher, S.B. Belhaouari, K. Deshmukh, C.M. Hussain, F.A Sharifianjazi, Magnetite composite of molecularly imprinted polymer and reduced graphene oxide for sensitive and selective electrochemical detection of catechol in water and milk samples: An artificial neural network (ANN) application, *Journal of The Electrochemical Society*. 170(4) (2023), 047502. doi:10.1149/1945-7111/acc97c
- [51] M.E. Pekdemir, S. Pekdemir, Ş. İnci, S. Kırbağ, M. Çiftci, Thermal, Magnetic properties and antimicrobial effects of magnetic iron oxide nanoparticles treated with *Polygonum cognatum*, *Iranian Journal of Science and Technology, Transactions of Civil Engineering*. 45 (5) (2021), 1579–1586. doi:10.1007/s40995-021-01167-4
- [52] R. Abaid, M. Malik, M.A. Iqbal, M. Malik, Z. Shahwani, T.Z. Ali, K. Morsy, R. Y. Capangpangan, A.C. Alguno, J.R. Choi, Biosynthesizing *Cassia fistula* extract-mediated silver nanoparticles for MCF-7 cell lines anti-cancer assay, *ACS Omega*. 8(19) (2023), 17317–17326. doi:10.1021/acsomega.3c02225
- [53] T.C. Kömürçü, N. Bilgiçli, Yumurtalı ve yumurtasız formüle edilen madımak (*Polygonum cognatum*) tozu ilaveli eriştelelerin fonksiyonel içeriği ve duyuşal özellikleri, *Necmettin Erbakan University Journal of Science and Engineering*. 6(1), (2024), 124-138. doi:10.47112/neufmbd.2024.37
- [54] P.N.V.K. Pallela, S. Ummey, L.K. Ruddaraju, S.V.N. Pammi, S.G Yoon, Ultra Small, mono dispersed green synthesized silver nanoparticles using aqueous extract of *Sida cordifolia* plant and investigation of antibacterial activity, *Microbial Pathogenesis*. 124 (2018), 63-69. doi:10.1016/j.micpath.2018.08.026
- [55] D. Nayak, S. Ashe, P.R. Rauta, M. Kumari, B. Nayak, Bark extract mediated green synthesis of silver nanoparticles: evaluation of antimicrobial activity and antiproliferative response against osteosarcoma, *Materials Science and Engineering:C*. 58 (2016), 44-52. doi:10.1016/j.msec.2015.08.022
- [56] J. Jiang, G. Oberdörster, P. Biswas, Characterization of size, surface charge, and agglomeration state of nanoparticle dispersions for toxicological studies, *Journal of Nanoparticle Research*. 11 (2009), 77-89. doi:10.1007/s11051-008-9446-4
- [57] X. Yin, W. Que, D. Fei, F. Shen, Q. Guo, Ag nanoparticle/ZnO nanorods nanocomposites derived by a seed-mediated method and their photocatalytic properties, *Journal of Alloys and Compounds*. 524 (2012), 13-21. doi:10.1016/j.jallcom.2012.02.052
- [58] N. Bhattacharjee, I. Som, R. Saha, S.A Mondal, critical review on novel eco-friendly green approach to synthesize zinc oxide nanoparticles for photocatalytic degradation of water pollutants, *International Journal of Environmental Analytical Chemistry*. 104(3) (2024), 489-516. doi:10.1080/03067319.2021.2022130
- [59] H. Jan, M. Shah, H. Usman, M.A. Khan, M. Zia, C. Hano, B.H. Abbasi, Biogenic synthesis and

- characterization of antimicrobial and antiparasitic zinc oxide (ZnO) nanoparticles using aqueous extracts of the Himalayan Columbine (*Aquilegia pubiflora*), *Frontiers in Materials*. 7 (2020), 249. doi:10.3389/fmats.2020.00249
- [60] A. Król, P. Pomastowski, K. Rafińska, V. Railean-Plugaru, B. Buszewski, Zinc oxide nanoparticles: Synthesis, antiseptic activity and toxicity mechanism, *Advances in colloid and interface science*. 249 (2017), 37-52. doi:10.1016/j.cis.2017.07.033
- [61] M. Bandeira, M. Giovanela, M. Roesch-Ely, D.M. Devine, J. da Silva Crespo, Green synthesis of zinc oxide nanoparticles: A review of the synthesis methodology and mechanism of formation, *Sustainable Chemistry and Pharmacy*. 15 (2020), 100223. doi:10.1016/j.scp.2020.100223
- [62] N. Singh, F.Z. Haque, Synthesis of zinc oxide nanoparticles with different pH by aqueous solution growth technique, *Optik*. 127(1) (2016). 174-177. doi:10.1016/j.ijleo.2015.09.024
- [63] T. Parsai, A. Kumar, Understanding effect of solution chemistry on heteroaggregation of zinc oxide and copper oxide nanoparticles, *Chemosphere*. 235 (2019), 457-469. doi:10.1016/j.chemosphere.2019.06.171
- [64] H. Veisi, S. Azizi, P. Mohammadi, Green synthesis of the silver nanoparticles mediated by *Thymra spicata* extract and its application as a heterogeneous and recyclable nanocatalyst for catalytic reduction of a variety of dyes in water, *Journal of Cleaner Production*. 170 (2018), 1536-1543. doi:10.1016/j.jclepro.2017.09.265
- [65] A. Dandia, S.L. Gupta, A. Indora, P. Saini, V. Parewa, K.S. Rathore, Ag NPs decked GO composite as a competent and reusable catalyst for 'ON WATER' chemoselective synthesis of pyrano [2, 3-c: 6, 5-c'] dipyrazol]-2-ones, *Tetrahedron Letters*. 58(12) (2017), 1170-1175. doi:10.1016/j.tetlet.2017.02.014
- [66] S.K. Pandey, M.K. Tripathi, V. Ramanathan, P.K. Mishra, D. Tiwary, Enhanced photocatalytic efficiency of hydrothermally synthesized g-C₃N₄/NiO heterostructure for mineralization of malachite green dye, *Journal of Materials Research and Technology*. 11 (2021), 970-981. doi:10.1016/j.jmrt.2021.01.059
- [67] C.W. Lou, A.P. Chen, T.T. Lic, J.H. Lin, Antimicrobial activity of UV-induced chitosan capped silver nanoparticles, *Materials Letters*. 128 (2014), 248-252. doi:10.1016/j.matlet.2014.04.145
- [68] M. Zafar, T. Iqbal, Green synthesis of silver and zinc oxide nanoparticles for novel application to enhance shelf life of fruits. *Biomass Conversion and Biorefinery*. 14(4) (2024), 5611-5626. doi:10.1007/s13399-022-02730-8
- [69] N. Ahmad, S. Sharma, M.K. Alam, V.N. Singh, S.F. Shamsi, B.R., Mehta, A. Fatma, Rapid synthesis of silver nanoparticles using dried medicinal plant of basil, *Colloids and Surfaces B: Biointerfaces*. 81(1) (2010), 81-86. doi:10.1016/j.colsurfb.2010.06.029
- [70] D.R. Mota, W.D.S. Martini, D.S. Pellosi, Influence of Ag size and shape in dye photodegradation using silver nanoparticle/ZnO nanohybrids and polychromatic light, *Environmental Science and Pollution Research*. 30(20) (2023), 57667-57682. doi:10.1007/s11356-023-26580-7
- [71] M.U. Rashid, S.J. Shah, S. Attacha, L. Khan, J. Saeed, S.T. Shah, H.I. Mohamed, Green Synthesis and characterization of zinc oxide nanoparticles using *Citrus limetta* peels extract and their antibacterial activity against brown and soft rot pathogens and antioxidant potential, *Waste and Biomass Valorization*. (2024), 1-16. doi:10.1007/s12649-023-02389-w
- [72] P. Perumal, N.A. Sathakkathulla, K. Kumaran, R. Ravikumar, J.J. Selvaraj, V. Nagendran, S. Rathinasamy, Green synthesis of zinc oxide nanoparticles using aqueous extract of shilajit and their anticancer activity against HeLa cells, *Scientific Reports*. 14(1) (2024), 2204. doi:10.1038/s41598-024-52217-x
- [73] P. Ramesh, A. Rajendran, M. Ashokkumar, Biosynthesis of zinc oxide nanoparticles from *Phyllanthus niruri* plant extract for photocatalytic and antioxidant activities, *International Journal of Environmental Analytical Chemistry*. 104(7) (2024), 1561-1572.

- doi:10.1080/03067319.2022.2041004
- [74] P.A. Luque, H.E. Garrafa-Gálvez, C.A. García-Maró, C.A. Soto-Robles, Study of the optical properties of ZnO semiconductor nanoparticles using *Origanum vulgare* and its effect in Rhodamine B degradation, *Optik*. 258 (2022), 168937. doi: 10.1016/j.ijleo.2022.168937
- [75] Md.R. Khan, S.M. Hoque, K.F.B. Hossain, Md.A.B. Siddique, Md.K. Uddin, Md.M. Rahman, Green synthesis of silver nanoparticles using *Ipomoea aquatica* leaf extract and its cytotoxicity and antibacterial activity assay, *Green Chemistry Letters and Reviews*. 13(4) (2020), 303-315. doi:10.1080/17518253.2020.1839573
- [76] K.J. Rao, S. Paria, Green synthesis of silver nanoparticles from aqueous *Aegle marmelos* leaf extract, *Materials Research Bulletin*. 48(2) (2013), 628-634. doi: 10.1016/j.materresbull.2012.11.035
- [77] D.A. Kumar, V. Palanichamy, S.M. Roopan, Green synthesis of silver nanoparticles using *Alternanthera dentata* leaf extract at room temperature and their antimicrobial activity, *Spectrochimica Acta Part A: Molecular and Biomolecular Spectroscopy*. 127 (2014), 168-171. doi: 10.1016/j.saa.2014.02.058
- [78] J.A. Garibay-Alvarado, M.A. Ruiz-Esparza-Rodríguez, E.A. Zaragoza-Contreras, S.Y. Reyes-López, Ag nanoparticle-decorated SiO₂-Al₂O₃-ZrO₂ composites as a low-cost substrate for enhanced signal infrared spectroscopy, *ACS Applied Nano Materials*. 7(5) (2024). 4658-4666. doi:10.1021/acsanm.3c03464
- [79] L. Gharibshahi, E. Saion, E. Gharibshahi, A.H. Shaari, K.A. Matori, Structural and optical properties of Ag nanoparticles synthesized by thermal treatment method, *Materials*. 10(4) (2017), 402. doi:10.3390/ma10040402
- [80] R.B. Patil, A.D. Chougale, Analytical methods for the identification and characterization of silver nanoparticles: A brief review, *Materials Today: Proceedings*. 47 (2021), 5520-5532. doi:10.1016/j.matpr.2021.03.384
- [81] S.K. Rout, B.C. Tripathy, P. Padhi, B.R. Kar, K.G. Mishra, A green approach to produce silver nano particles coated agro waste fibers for special applications, *Surfaces and Interfaces*. 7 (2017), 87-98. doi:10.1016/j.surfin.2017.03.004
- [82] S. Ahmad, A. Yousaf, M.N. Tahir, A.A. Isab, M. Monim-ul-Mehboob, W. Linert, M. Saleem, Structural characterization and antimicrobial activity of a silver (I) complex of arginine, *Journal of Structural Chemistry*. 56 (2015), 1653-1657. doi:10.1134/S0022476615080302
- [83] V.P. Singh, D. Das, C. Rath, Studies on intrinsic defects related to Zn vacancy in ZnO nanoparticles, *Materials Research Bulletin*. 48(2) (2013), 682-686. doi:10.1016/j.materresbull.2012.11.026
- [84] A.M. Mostafa Mwafy, A. Eman, A.M. Khalil, A. Toghan, E.A. Alashkar, ZnO/Ag multilayer for enhancing the catalytic activity against 4-Nitrophenol, *Journal of Materials Science: Materials in Electronics*. 34(4) (2023), 300. doi:10.1007/s10854-022-09631-6
- [85] Y. Sun, W. Zhang, Q. Li, H. Liu, X. Wang, Preparations and applications of Zinc Oxide based photocatalytic materials, *Advanced Sensor and Energy Materials*. 2(3) (2023), 100069. doi: 10.1016/j.asems.2023.100069
- [86] J. Bednář, L. Svoboda, Z. Rybková, R. Dvorský, K. Malachová, T. Stachurová, D. Matýsek, V. Foldyna, Antimicrobial synergistic effect between Ag and Zn in Ag-ZnO·mSiO₂ silicate composite with high specific surface area, *Nanomaterials (Basel)*. 9(9) (2019), 1265. doi: 10.3390/nano9091265
- [87] M. Şahin, Y. Arslan, F. Tomul, B. Yıldırım, H. Genç, Green synthesis of silver nanoparticles using *Lathyrus brachypterus* extract for efficient catalytic reduction of methylene blue, methyl orange, methyl red and investigation of a kinetic model, *Reaction Kinetics, Mechanisms and Catalysis*. 135(6) (2022), 3303-3315. doi:10.1007/s11144-022-02299-3

- [88] M. Rafique, I. Sadaf, M.B. Tahir, M.S. Rafique, G. Nabi, et al. Novel and facile synthesis of silver nanoparticles using *Albizia procera* leaf extract for dye degradation and antibacterial applications, *Materials Science and Engineering: C*. 99 (2019), 1313–1324. doi:10.1016/j.msec.2019.02.059
- [89] H.T. Kahraman, Synthesis of silver nanoparticles using *Alchemilla vulgaris* and *Helichrysum arenarium* for methylene blue and 4-nitrophenol degradation and antibacterial applications, *Biomass Conversion and Biorefinery*. (2024), 1-12. doi:10.1007/s13399-024-05314-w
- [90] K. Naseem, M. Zia Ur Rehman, A. Ahmad, D. Dubal, T.S. AlGarni, Plant extract induced biogenic preparation of silver nanoparticles and their potential as catalyst for degradation of toxic dyes, *Coatings*. 10 (2020), 1235. doi:10.3390/coatings10121235
- [91] P.K. Pandey, J. Sarkar, S. Srivastava, Catalytic dye degradation of textile dye methylene blue by using silver nanoparticles fabricated by sustainable approach, *Engineering Proceedings*. 37(1) (2023), 16. doi:10.3390/ECP2023-14684
- [92] A. Yeganeh-Faal, M. Bordbar, N. Negahdar, M. Nasrollahzadeh, Green synthesis of the Ag/ZnO nanocomposite using *Valeriana officinalis* L. root extract: application as a reusable catalyst for the reduction of organic dyes in a very short time, *Iet Nanobiotechnology*. 11(6) (2017), 669-676. doi:10.1049/iet-nbt.2016.0198
- [93] R. Rajasekar, R. Thanasamy, M. Samuel, T.N.J.I. Edison, N. Raman, Ecofriendly synthesis of silver nanoparticles using *Heterotheca subaxillaris* flower and its catalytic performance on reduction of methyl orange, *Biochemical Engineering Journal*. 187 (2022), 108447. doi:10.1016/j.bej.2022.108447
- [94] K. Nagaraj, P. Thangamuniyandi, S. Kamalesu, M. Dixitkumar, A.K. Saini, S.K. Sharma, C. Karuppiah, Silver nanoparticles using *Cassia alata* and its catalytic reduction activities of rhodamine6G, methyl orange and methylene blue dyes, *Inorganic Chemistry Communications*. 155 (2023), 110985. doi:10.1016/j.inoche.2023.110985
- [95] D. Khwannimit, R. Maungchang, P. Rattanakit, Green synthesis of silver nanoparticles using *Clitoria ternatea* flower: an efficient catalyst for removal of methyl orange, *International Journal of Environmental Analytical Chemistry*. 102(17) (2022), 5247-5263. doi:10.1080/03067319.2020.1793974
- [96] V.V. Konduri, N.K. Kalagatur, L. Gunti, U.K. Mangamuri, V.R. Kalagadda, S. Poda, S.B.N. Krishna, Green synthesis of silver nanoparticles from *Hibiscus tiliaceus* L. Leaves and their applications in dye degradation, antioxidant, antimicrobial, and anticancer activities, *South African Journal of Botany*. 168 (2024), 476-487. doi:10.1016/j.sajb.2024.03.035
- [97] B.U. Hijazi, M. Faraj, R. Mhanna, M.H. El-Dakdouki, Biosynthesis of silver nanoparticles as a reliable alternative for the catalytic degradation of organic dyes and antibacterial applications, *Current Research in Green and Sustainable Chemistry*. 8 (2024), 100408. doi:10.1016/j.crgsc.2024.100408